

IDŐJÁRÁS

*Quarterly Journal of the Hungarian Meteorological Service
Vol. 121, No. 1, January – March, 2017, pp. 1–28*

Numerical simulation of sulfate formation in water drops: results of a box experiment

Gabriella Schmeller^{1*} and István Geresdi²

¹*University of Pécs, Faculty of Sciences
Doctoral School of Earth Sciences
Ifjúság útja 6, 7624 Pécs, Hungary
E-mail: schg@gamma.ttk.pte.hu*

²*University of Pécs, Faculty of Sciences
Institute of Geography
Ifjúság útja 6, 7624 Pécs, Hungary
E-mail: geresdi@gamma.ttk.pte.hu*

**Corresponding author*

(Manuscript received in final form May 31, 2016)

Abstract—The purpose of the research was to investigate how sulfate formation depends on the drop size, and to find efficient scheme for the numerical integration of ODEs (ordinary differential equations) describing absorption and chemical reactions. A box model was developed to simulate how the water drops absorb the different compounds and to simulate formation of sulfate by oxidation processes. Results show, that the length of time step necessary for the accurate integration of the differential equation depends on the drop size and on the concentration of the trace gases in the environment of the water drop. Analysis of the data suggests that the time step should be at least 0.01 s if the drop size is smaller than 20 μm , and it can be 0.1 s above this size. The time evolution of the pH of solution and that of the concentration of different compounds inside of water drops significantly depend on the size of the drops. In the case of water drops smaller than 50 μm , the concentration of the compounds becomes steady state in time interval less than 20 s, that is absorption and oxidation processes occur at almost same rate. In the case of larger drops, it takes significantly longer time to reach this balance. In the polluted atmosphere, the mass of the condensation nuclei can increase significantly due to the chemical processes occurring inside of the water drops. The results of this research will be used in a two-dimensional model simulating these processes in stratocumulus clouds with bin microphysical scheme.

Key-words: cloud chemistry, numerical simulation, absorption, oxidation, sulfate formation

1. Introduction

The investigation of the chemical composition of rainwater has got into the focus of the research about atmospheric chemistry in the last decades. From the middle of the last century, the air pollution caused by the industry, traffic, agriculture, as well as households has endangered the natural environment and the human health. The increasing occurrence of acid rain and heavy air pollution related to smog have initiated researches about the role of cloud and precipitation elements in the accumulation of the pollution in the atmosphere and on the surface.

The emitted air pollutants show vertical and horizontal inhomogeneities in the atmosphere that depend on the characteristics of the emission (e.g., location and intensity of emission and chemical properties of the pollutants), the surface (topography), and atmosphere (e.g., temperature profile, wind speed, and cloud cover). The chemically inert gases can reach the stratosphere and can be transported to huge distances. The chemically active gases get into reactions with other chemicals both in gas and liquid phases. The rate of reaction depends on the characteristics of the atmospheric environment such as temperature, pressure, and relative humidity; and furthermore, on the type of the reaction. The liquid and solid phase hydrometeors not only absorb or desorb gases, but also numbers of chemical reactions can occur in these particles. This is the reason why clouds and precipitation play an important role in the transport (both in vertical and horizontal directions) and in the washout of air pollutants compounds. Broad scale of processes – from absorption of gases in micron-size water drops to transport of particles by kilometer-size updraft core – have to be studied to clarify the role of clouds in the transport of pollutants.

A number of researches over the past few decades have focused on the absorption of different trace gases by water drops, especially sulfur-dioxide (SO_2) and different oxidizing compounds, furthermore on the description of their chemical properties and reactions. *Diehl et al.* (2000) gives a comprehensive summary about the most important theoretical and laboratory studies and about the results of field experiments that have been accomplished. In the beginning of the 1980's, numerous field studies (e.g., *Hegg and Hobbs*, 1981, 1982; *Daum et al.*, 1983; *Hegg et al.*, 1984; *Barrie*, 1985) proved that a significant fraction (~ 60%) of sulfate (SO_4^{2-}) in drops is produced by absorption of sulfur-dioxide and converting it into sulfate by several chemical reactions, and the other part was formed by dissolution of aerosol particles.

Field measurements and chemical analysis of the collected precipitation samples gave a comprehensive overview about the chemical components inside the cloud and precipitation elements. These studies gave a correct description about the transport of pollutants in the lower atmosphere, but they provided less detail about physical and chemical processes occurring inside of water drops, and on the surface of ice particles.

A number of laboratory observations have been accomplished to study absorption and desorption of gases in water drops and on the surface of ice particles. Based on laboratory studies *Beilke and Georgii, 1968, Beilke, 1970, Barrie and Georgii, 1976, and Walcek et al., 1984* asserted, that the amount of absorbed SO₂ increased with increasing gas concentration and with the exposure time of the gas. It was asserted that molar concentration of SO₂ in water drops could reach a limiting equilibrium value if only SO₂ gas is present for long time period. In the case of drops smaller than diameter of 20 μm the solution is always in equilibrium with the gas phase in the environment. Chemical processes, e.g., dissociation of absorbed gases, oxidation of ions and the change of pH of solution have been investigated by several researchers. *Beilke et al. (1975)* determined the oxidation rate of dissolved 4-valence sulfur S(IV) species ($(\text{SO}_2)_{\text{aq}}$, HSO_3^- , and SO_3^{2-}) to 6-valence sulfur S(VI) species (HSO_4^- and SO_4^{2-}) in pure water drops. This rate was found to be rather slow ($\sim 10^{-5} \% \text{ h}^{-1}$). *Seinfeld (1986)* showed that other chemical species can be also found in water drops, and some types of compounds may act as oxidizing agents (e.g., hydrogen-peroxide (H₂O₂) and ozone (O₃)). In drops containing these oxidizing agents, the total amount of sulfur in the liquid phase is continuously increasing with time (*Walcek et al., 1984; Waltrop et al., 1991*).

As a new research tool, numerical models have been developed to study the uptake of trace gases by water drops and the chemical reactions that occur inside of water drops. The results of these models have been verified mostly by laboratory experiments.

Description of absorption of gases into and out of water drops has been continuously improved since the middle of the last century. *Kronig and Brink (1950), Kronig et al. (1951), Johnson et al. (1967), and Watada et al. (1970)* solved the equation describing the convective diffusion inside the drop. *Walcek and Pruppacher (1984)* took into account the internal circulation in numerical simulation of diffusion of sulfur-dioxide occurred across the air-water interface. *Waltrop et al. (1991), Mitra et al. (1992), Hannemann et al. (1995, 1996), and Diehl et al. (2000)* carried out several laboratory experiments in a vertical wind tunnel and compared the results of observation with that of theoretical models. The unique of this type of measurement is that the drops are freely suspended in the vertical wind tunnel due to laminar or turbulent air flow, which mimics atmospheric conditions (*Diehl et al., 2011*). In their laboratory experiments, *Waltrop et al. (1991)* investigated the uptake of SO₂ from the gas phase in the presence of H₂O₂ in the liquid phase. A simplified version of the theoretical model published by *Walcek and Pruppacher (1984)* was used (model for well-mixed drop) for the prediction of SO₂ diffusion into water drops. *Waltrop et al. (1991)* and *Mitra and Hannemann (1993)* published details about the equations used in the well-mixed model. In the case of millimeter sized drops, the results

of the laboratory experiments were in good agreement with that of the well-mixed model.

Hannemann et al. (1995, 1996) investigated the uptake and desorption of ammonia (NH_3) in the presence of carbon-dioxide (CO_2) and the simultaneous uptake of NH_3 , SO_2 and CO_2 , by water drops by using realistic vertical profile of these gases. In both cases the observed data agreed well with the results of the well-mixed model and with that of the Kronig-Brink model (details by *Walcek and Pruppacher*, 1984), that gives a sophisticated description about gas diffusion inside the drop. *Hannemann et al.* (1995) asserted that the slow hydration reaction of CO_2 must be taken into consideration in the model calculations, otherwise the amount of NH_3 is significantly overestimated. The model calculations were verified by observation of the simultaneous uptake of NH_3 , SO_2 , and CO_2 (*Hannemann et al.*, 1996). Important results were that the uptake of SO_2 strongly depended on the concentration of NH_3 and on the precipitation intensity, furthermore, they proved that if NH_3 and SO_2 are simultaneously present, their desorption is negligible. They also found that, the small drops more efficiently wash out these gases than the larger ones.

Several authors studied the role of ice crystals in the uptake and retention of trace gases (*Diehl et al.*, 1998; *v. Blohn et al.*, 2013), and also numerical models have been developed to study this process in the case of frozen drops (*Stuart and Jacobson*, 2005). They also proved that the direct uptake of gases by ice particles is not as efficient as by water drops. The most effective process to uptake of gases by ice particles is the riming.

In Hungary, the first attempts about precipitation chemistry were made in the early 60th. The setting of the surface network allowed the observation of chemical characteristics of precipitation (e.g., pH, electrical conductivity, sodium, potassium, magnesium, calcium, ammonium, sulfate, nitrate, nitrite, chloride, and orthophosphate ion content). The early precipitation chemistry measurements were accomplished by open samplers, which frequently overestimated the concentration of different ions by 100%. To avoid this high sampling failure rate, an automatic sampling network was established (*Horváth*, 1981). The accuracy of the data measured by this network – using automatic collectors - was analyzed in the early 80th. A suggestion for the development of the precipitation chemistry station was published to significantly improve the spatial resolution of the observations in Hungary. The dramatically increased air pollution in Hungary initiated comprehensive researches about the atmospheric and precipitation chemistry in the early 70th. *Mészáros* (1976) studied the sources, concentration, and chemical reactions of sulfur-dioxide, furthermore the chemical composition of background aerosol particles. Observations, accomplished in different regions of the world, showed that the concentration of sulfur-dioxide strongly decreases as the distance from the source increases, and that the relative amount of sulfate related to sulfur-dioxide increases. This phenomenon can be explained partly by the removal of sulfur-dioxide from the

atmosphere and partly by the efficient conversion of sulfur-dioxide to sulfate or to other compounds. This process was widely observed during field measurement campaigns. *Mészáros* (1973, 1974) published results about the correlation between the sulfate concentration and different atmospheric parameters. They asserted that sulfate aerosol particles formed in different ways during summer and during winter. *Mészáros* and *Vissz* (1974) studied the properties of aerosol particles over the oceans in the southern hemisphere. They observed that the aerosol particles in the maritime air mass mainly consist of ammonium sulfate ($(\text{NH}_4)_2\text{SO}_4$) and mixture of ammonium sulfate and sea salt. *Mészáros* (1976) concluded that aside from the sea salt, the tropospheric background aerosol mainly consists of sulfur compounds.

Várhelyi (1977, 1980, 1982) developed several numerical models to simulate the annual (or daily) variation of sulfur budget over Hungary, and to estimate rainout and washout of sulfate particles and sulfur-dioxide. She compared the simulated data with data of field observations. The analysis of the data showed that while both in-cloud scavenging (washout) and below-cloud scavenging (rainout) played important role in the wet removal of SO_2 , sulfate particles were mostly washed out by cloud droplets. NH_3 has a significant role in the wet removal of SO_2 .

Numerous calculations were made to simulate the chemical processes occurring in water drops. *Horváth* and *Mészáros*. (1978) and *Horváth* (1977) determined the mechanisms and kinetic parameters for sulfur-dioxide to sulfate conversion. *Horváth et al.* (1978) determined the rate constant for sulfur-sulfate oxidation occurring during summer and in two seasons (winter + summer). The results showed that the transformation of SO_2 is slower during summer than during winter. *Várhelyi* (1975) published results about the development of a numerical model to simulate the absorption and oxidation of sulfur-dioxide in cloud and fog droplets in the presence of ammonia.

In the middle of the seventies, several research projects have been accomplished to study the characteristics of sulfate-particles in the lower troposphere, such as the size distribution, concentration, and residence time (*Mészáros* and *Várhelyi*, 1975). The calculation of condensational growth of cloud droplets on ammonium sulfate particles was studied by *Mészáros et al.* (1974). The concentration and distribution of CCN (cloud condensation nuclei) containing ammonium sulfate was established referring to the results of field measurements. The effect of oxidation of SO_2 inside of water drops on the growth of sulfate condensation nuclei was also studied by numerical simulations (*Várhelyi*, 1975). *Mészáros* and *Várhelyi*, (1975) concluded from the observation data that on regional scale, most of the sulfate particles are smaller than $0.2 \mu\text{m}$. They also argued that wet deposition removed the sulfate particles from the atmosphere more efficiently than dry deposition. *Mészáros et al.* (1974) investigated how the characteristics of aerosol particles (act as condensation nuclei) affect the evolution of size distribution of water drops. These aerosol particles were classified in different categories according to their

mass and their effect on water drop concentration. *Várhelyi* (1975) found that the calculated radius of ammonium sulfate particles was in good agreement with the observed values, furthermore, the oxidation of SO₂ in the presence of NH₃ in cloud and fog droplets is one of the main processes producing ammonium sulfate particles. Comparison of the simulated size distributions with the observation data published by *Mészáros* (1971) showed a bias between the predicted (0.3 – 0.6 μm) and measured (< 0.1 – 3 μm) size ranges. This discrepancy made her to suggest, that other chemical reaction might take part in the formation of ammonium sulfate particles besides the oxidation of SO₂ occurring inside of the water drops as well.

2. Description of the model

A box model was developed to simulate physical and chemical processes occurring in clouds. This type of box model does not allow us to simulate the scavenging of gases. The focus of our research is on looking for accurate and efficient solution of the ordinary differential equations (ODEs) describing the absorption/desorption of chemical compounds through the surface of water drops, furthermore for that of chemical reactions equations for water drops, especially the oxidation mechanisms of sulfur-dioxide producing sulfate ions. Sensitivity test was made by repeating the numerical experiments at six different drop sizes (10 μm, 20 μm, 50 μm, 70 μm, 100 μm, and 500 μm). The diffusional growth of water drops and the accretion by collision-coalescence were not taken into consideration. The role of chemical characteristics and atmospheric concentration of the compounds of CO₂, SO₂, NH₃, O₃, and H₂O₂ were investigated in the formation of sulfate inside water drops of different sizes. In the presence of ammonium ion (NH₄⁺), the effect of acidic compounds on the pH is compensated, and ammonium sulfate particles may form after the evaporation of water drops. Some oxidizing agents, e.g., ozone (O₃) and hydrogen-peroxide (H₂O₂) can also promote this process through pH-dependent reactions. Their concentration in the solution depends on their amount in the gas phase, on their chemical properties (e.g., Henry's law constant and dissociation constant), and on the size of the drops. The dissociation constants of these gases depend on the pH of the solution. There is also a strong interaction between the hydrogen ion concentration and the rate of chemical reactions. These are only a few examples of that the gases and the liquid water drops form rather complex chemical system. This complexity is enhanced by the size dependence of absorption rates and by that of the rates of chemical reactions.

The uptake of gases by water drops was calculated by a model, assuming that the compounds are well-mixed inside of water drops all the time. The diffusion of gases through the surface of water drops is given by the following formula (*Pruppacher and Klett, 2010*):

$$\frac{dc_l}{dt} = \frac{3 \cdot D_g}{r^2} \left(c_{g,\infty} - \frac{c_l}{K_H^* \cdot R \cdot T} \right) \cdot f_v, \quad (1)$$

where c_l and $c_{g,\infty}$ are the gas concentration inside of the drop and far from the drop in M [mole litre⁻¹] and ppbv, respectively; D_g is the diffusion constant in m² s⁻¹ depending on the type of the gas and on the temperature; r is the radius of the drop in m, f_v is the ventilation coefficient, K_H^* is the modified (due to the dissociation) Henry's law constant in M Pa⁻¹, $R = 8.2 \cdot 10^3$ Pa M⁻¹ K⁻¹, and T is the temperature in units of K. The dependence of the K_H^* on the pH of the solution is shown in Fig. 1. Low dissociation rate of the H₂O₂ reflects that K_H^* only slightly depends on the pH. In the case of CO₂, the K_H^* remains near constant only if the pH is less than 5.0. K_H^* strongly depends on pH both in the cases of SO₂ and NH₃. The plots in Fig. 1 also suggest that NH₃ is more efficiently absorbed at low pH values than at larger ones, and vice versa, SO₂ is more efficiently absorbed at larger pH values than at smaller ones.

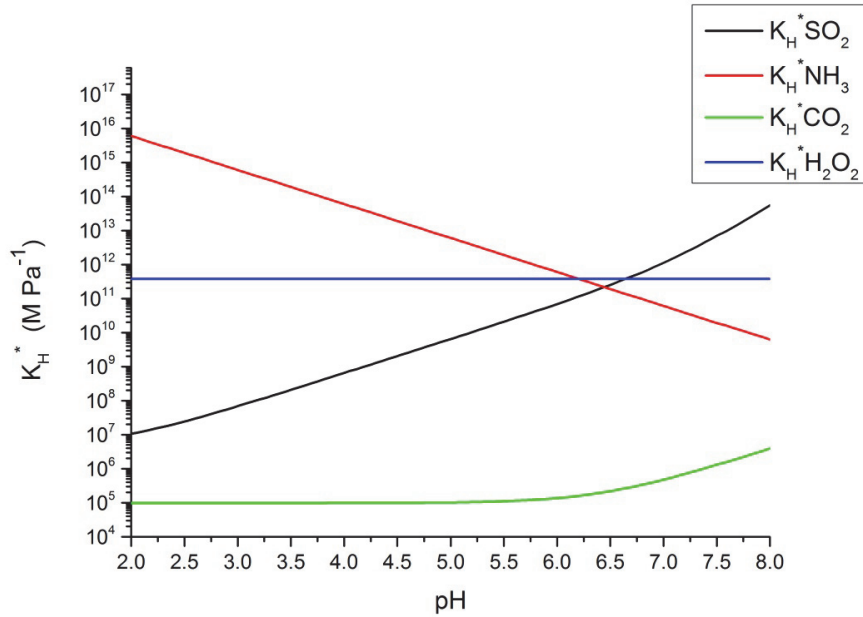


Fig. 1. Dependence of modified Henry's law constant (K_H^*) on pH in the case of different compounds.

If the dissolved gases completely dissociate in the drop, $k_H^* = k_H \cdot K_1 / c_l$, for $[H^+] \ll K_1$ and $[H^+] \approx c_l$, where k_H^* and k_H are dimensionless and considered as $k_H = K_H \cdot R \cdot T$ with $R = 8.2 \cdot 10^3$ Pa M⁻¹ K⁻¹. T is the temperature in units of K, $[H^+]$ is the hydrogen ion concentration in M, K_H is the Henry's law constant in M Pa⁻¹, and K_1 is the dissociation constant of the given chemical species in water in M. In this case Eq. (1) can be modified into the following form:

$$\frac{dc_l}{dt} = \frac{3 \cdot D_g}{r^2} \left(c_{g,\infty} - \frac{c_l^2}{k_H \cdot K_1} \right) \cdot f_v. \quad (2)$$

The advantage of this equation is that it does not involve the pH dependence of the modified Henry's law constant, so it can be solved analytically for the gases whose K_H^* depends on the pH. Unfortunately, the above mentioned conditions are not fulfilled for NH_3 and CO_2 .

The oxidation mechanism of S(IV) species to S(VI) by O_3 and H_2O_2 are calculated by the formulas given by *Seinfeld and Pandis (2006)*. H_2O_2 is a very soluble gas in water, and under typical atmospheric conditions, the OH radical produced from H_2O_2 oxidizes mainly the HSO_3^- ions as principal reactive S(IV) species (*McArdle and Hoffmann, 1983*). So the rate of oxidation can be given by the following equation (*Hoffmann and Calvert, 1985*):

$$-\frac{d[S(IV)]}{dt} = \frac{k \cdot [H^+] \cdot [H_2O_2] \cdot [HSO_3^-]}{1 + K \cdot [H^+]}, \quad (3)$$

where $k = 7.5 \pm 1.16 \cdot 10^7 \text{ M}^{-2} \text{ s}^{-1}$ and $K = 13 \text{ M}^{-1}$ at 298 K. The concentration of HSO_3^- ion can be given as a function of absorbed SO_2 (sum of $[(\text{SO}_2)_{\text{aq}}]$, $[\text{HSO}_3^-]$ and $[\text{SO}_3^{2-}]$):

$$[\text{HSO}_3^-] = \frac{[S(IV)]}{\left[1 + \frac{[H^+]}{K_1} + \frac{K_2}{[H^+]} \right]}, \quad (4)$$

where K_1 and K_2 are the first and second dissociation constants of $(\text{SO}_2)_{\text{aq}}$ in unit of M, respectively. Substituting Eq. (4) into Eq. (3) the oxidation rate can be given as a function of the concentration of absorbed H_2O_2 and SO_2 :

$$-\frac{d[S(IV)]}{dt} = \frac{k \cdot [H^+] \cdot [H_2O_2] \cdot [S(IV)]}{(1 + K \cdot [H^+]) \cdot \left(1 + \frac{[H^+]}{K_1} + \frac{K_2}{[H^+]} \right)} = [H_2O_2] \cdot [S(IV)] \cdot \frac{k \cdot [H^+]}{(1 + K \cdot [H^+]) \cdot \left(1 + \frac{[H^+]}{K_1} + \frac{K_2}{[H^+]} \right)}. \quad (5)$$

The aqueous phase concentration of H_2O_2 is about six orders of magnitude higher than that of O_3 under typical ambient conditions. Although it dissolves fast, its dissociation constant is rather small ($1.58 \cdot 10^{-12}$).

O₃ reacts in a different way with S(IV) species, than the H₂O₂ does. Oxidation reaction occurs with SO₃²⁻ with HSO₃⁻ and (SO₂)_{aq} as well. The oxidation rate of O₃ is increasing by increasing pH, as it follows the presence of the above mentioned ions. It can oxidize all S(IV) species (*Seinfeld and Pandis, 2006*):

$$-\frac{d[S(IV)]}{dt} = \left(k_0 \cdot [(SO_2)_{aq}] + k_1 \cdot [HSO_3^-] + k_2 \cdot [SO_3^{2-}] \right) \cdot [O_3] \quad (6)$$

The concentration of (SO₂)_{aq}, HSO₃⁻, and SO₃²⁻ ions can be given as a function of the absorbed SO₂:

$$[(SO_2)_{aq}] = \frac{[S(IV)]}{\left[1 + \frac{K_1}{[H^+]} + \frac{K_1 \cdot K_2}{[H^+]^2} \right]} \quad (7)$$

$$[HSO_3^-] = \frac{[S(IV)]}{\left[1 + \frac{[H^+]}{K_1} + \frac{K_2}{[H^+]} \right]} \quad (8)$$

$$[SO_3^{2-}] = \frac{[S(IV)]}{\left[1 + \frac{[H^+]}{K_2} + \frac{[H^+]^2}{K_1 \cdot K_2} \right]} \quad (9)$$

Substituting Eqs. (7), (8), and (9) into Eq. (6), the oxidation rate can be given as a function of the concentration of absorbed O₃ and that of absorbed SO₂:

$$-\frac{d[S(IV)]}{dt} = \left(k_0 \cdot \frac{[S(IV)]}{\left[1 + \frac{K_1}{[H^+]} + \frac{K_1 \cdot K_2}{[H^+]^2} \right]} + k_1 \cdot \frac{[S(IV)]}{\left[1 + \frac{[H^+]}{K_1} + \frac{K_2}{[H^+]} \right]} + k_2 \cdot \frac{[S(IV)]}{\left[1 + \frac{[H^+]}{K_2} + \frac{[H^+]^2}{K_1 \cdot K_2} \right]} \right) \cdot [O_3] = \quad (10)$$

$$[S(IV)] \cdot [O_3] \cdot \left(\frac{k_0}{\left[1 + \frac{K_1}{[H^+]} + \frac{K_1 \cdot K_2}{[H^+]^2} \right]} + \frac{k_1}{\left[1 + \frac{[H^+]}{K_1} + \frac{K_2}{[H^+]} \right]} + \frac{k_2}{\left[1 + \frac{[H^+]}{K_2} + \frac{[H^+]^2}{K_1 \cdot K_2} \right]} \right)$$

Using Eq. (5) and Eq. (10), the coefficients for oxidation rates can be plotted as the function of the pH (*Fig. 2.*).

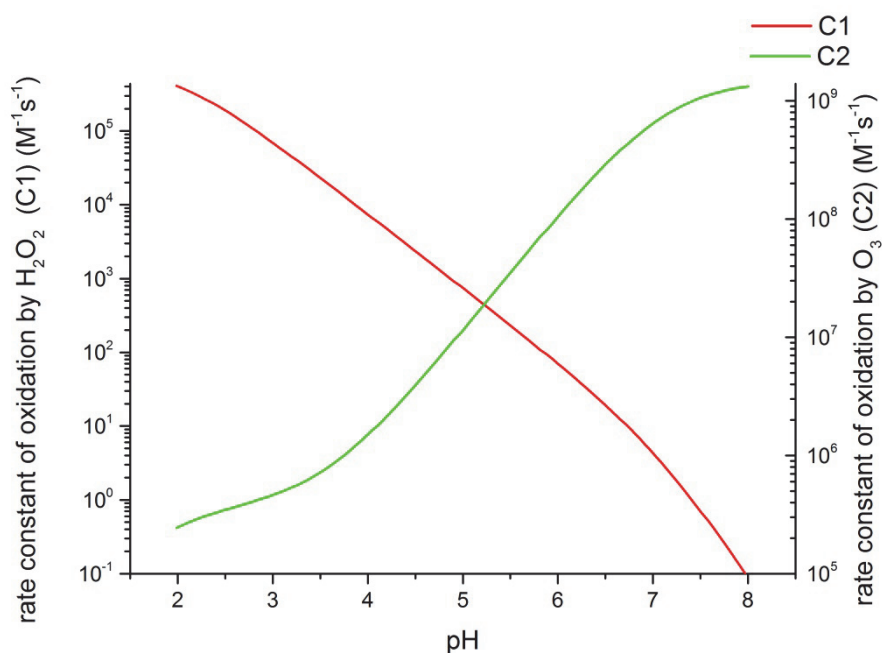


Fig. 2. The dependence of rate constants of S(IV) to S(VI) oxidation on the pH in the cases of oxidation by O₃ (green curve) and by H₂O₂ (red curve).

Although the rate constant related to the oxidation by O₃ is about five orders larger than in the case of oxidation by H₂O₂, the oxidation rate by H₂O₂ is about one-two orders larger, because the concentration of the H₂O₂ inside the water drops is about six orders larger than the concentration of O₃.

2.1. Description of the numerical techniques

Numerical modeling of absorption and that of chemical reactions occurring inside of water drops is a rather complex issue. The absorption/desorption rate of gases depends not only on their concentration in the ambient atmosphere, but on the turbulent mixing of the gases inside of the water drops, and the value of pH also affects the uptake of gases. The accurate and efficient numerical solution of the coupled differential equations describing the chemical reactions is also crucial. In the next phase of the research, we intend to implement these processes in a numerical cloud model, so it is important to find efficient numerical technique to solve the equations describing the above mentioned processes. Because both the rate of absorption and that of chemical reactions are sensitive on the value of pH, the accurate calculation of this diagnostic variable is also important.

2.1.1. Numerical solution of the absorption equations

In the case of O₃ and H₂O₂ gases, the analytical solution of Eq. (1) is possible because of the absence of dissociation (O₃) or due to very small dissociation rate (H₂O₂). The analytical solution of Eq. (2) can be applied to give the amount of absorbed SO₂ at some environmental conditions. Unfortunately, in the case of NH₃ and CO₂, there is no analytical solution to describe their absorption/desorption. In their cases, the numerical solution of Eq. (1) is used to evaluate the amount of the absorbed gases.

The Euler method is rather frequently applied for the solution of ordinary differential equations (ODEs) like Eq. (1). In this method, it is supposed that neither the concentration of dissolved gases in the liquid phase (c_l), nor the value of K_H^* change during the time step of Δt . The disadvantage of this method is that the above mentioned conditions can be hold if the time step used for integration is small enough. The other problem about the Euler method is that it causes large numerical dispersion (Geresdi and Weidinger, 1989).

To avoid these problems, a quasi-analytical method was chosen to solve Eq. (1). In this case, only the concentration of the hydrogen ions is supposed to remain constant during the time step of Δt , and by the end of the time step, the concentration of the gases in the liquid drop (c_l) is given by the following equation:

$$c_l(t + \Delta t) = c_{l,sat} - (c_{l,sat} - c_l(t)) \cdot e^{-const \cdot \Delta t}, \quad (11)$$

where $c_{l,sat}$ is the so called saturated concentration of the gas inside of the water drops in M:

$$c_{l,sat} = K_H^* \cdot R \cdot T \cdot c_g, \quad (12)$$

where c_g is the initial gas concentration inside of the drop in M calculated from the gas mixing ratio in the environment and the parameter $const$ in s⁻¹ is given by:

$$const = D_g \cdot \frac{3 \cdot f_v}{r^2 \cdot K_H^* \cdot R \cdot T}, \quad (13)$$

where D_g is the diffusion constant in m² s⁻¹; f_v is the ventilation coefficient, r is the radius of the drop in m, K_H^* is the modified Henry's law constant in M Pa⁻¹, $R = 8.2 \cdot 10^3$ Pa M⁻¹ K⁻¹, and T is the temperature in units of K.

Stability of this type of solution was investigated at different drop sizes and by varying the concentration of different gases in the ambient air. *Table 1*

summarizes the investigated cases and contains the time steps that are necessary to use for the accurate solution of Eq. (1) different drop sizes and at different environmental conditions. The calculations were repeated at three different time steps (1.0, 0.1, and 0.01 s). The data suggest that the time step has to be as small as 0.1 s. Even more, in some cases smaller time step (0.01 s) is necessary for the stable solution.

Table 1. Critical time steps (s) for numerical solution of differential equations describing the absorption of different trace gases at different drop sizes.

Case	Mixing ratio [ppbv]				Drop size [μm]					
	SO ₂	NH ₃	O ₃	H ₂ O ₂	10	20	50	70	100	500
					time step (s)					
01a	0.1	1	2	2	10 ⁻²	10 ⁻¹	10 ⁻¹	10 ⁻¹	10 ⁻¹	10 ⁻¹
1a	1	2	2	2	10 ⁻²	10 ⁻¹	10 ⁻¹	10 ⁻¹	10 ⁻¹	10 ⁻¹
2a	2	0	2	0	10 ⁻¹	10 ⁻¹	10 ⁻¹	10 ⁻¹	10 ⁻¹	10 ⁻¹
2b	2	0	2	2	10 ⁻¹	10 ⁻¹	10 ⁻¹	10 ⁻¹	10 ⁻¹	10 ⁻¹
2c	2	5	2	2	10 ⁻²	10 ⁻²	10 ⁻¹	10 ⁻¹	10 ⁻¹	10 ⁻¹
4a	4	2	2	2	10 ⁻¹	10 ⁻¹	10 ⁻¹	10 ⁻¹	10 ⁻¹	10 ⁻¹
5a	5	0	2	2	10 ⁻¹	10 ⁻¹	10 ⁻¹	10 ⁻¹	10 ⁻¹	10 ⁻¹
5b	5	2	2	0	10 ⁻¹	10 ⁻¹	10 ⁻¹	10 ⁻¹	10 ⁻¹	10 ⁻¹
5c	5	2	2	2	10 ⁻¹	10 ⁻¹	10 ⁻¹	10 ⁻¹	10 ⁻¹	10 ⁻¹
5d	5	5	2	2	10 ⁻²	10 ⁻¹	10 ⁻¹	10 ⁻¹	10 ⁻¹	10 ⁻¹
10a	10	5	2	2	10 ⁻¹	10 ⁻¹	10 ⁻¹	10 ⁻¹	10 ⁻¹	10 ⁻¹
20a	20	10	2	2	10 ⁻¹	10 ⁻¹	10 ⁻¹	10 ⁻¹	10 ⁻¹	10 ⁻¹
30a	30	10	2	2	10 ⁻²	10 ⁻¹	10 ⁻¹	10 ⁻¹	10 ⁻¹	10 ⁻¹
50a	50	10	2	2	10 ⁻²	10 ⁻¹	10 ⁻¹	10 ⁻¹	10 ⁻¹	10 ⁻¹

2.1.2. Numerical solution of the chemical reaction equations

A quasi-analytical method was applied to solve the ordinary differential equations (Eqs. (5) and (10)) describing the oxidation processes occur inside of water drops:

$$\int_{[S(IV)]_0}^{[S(IV)]} \frac{d[S(IV)]}{[S(IV)]} = \int_{t_0}^{t_0+\Delta t} -C_1 \cdot [H_2O_2]_{t_0} \cdot \Delta t, \quad (15)$$

$$\int_{[S(IV)]_0}^{[S(IV)]} \frac{d[S(IV)]}{[S(IV)]} = \int_{t_0}^{t_0+\Delta t} -C_2 \cdot [O_3]_{t_0} \cdot \Delta t, \quad (16)$$

where $C_1 = \frac{k \cdot [H^+]}{(1 + K \cdot [H^+]) \cdot \left(1 + \frac{[H^+]}{K_1} + \frac{K_2}{[H^+]}\right)}$ is from Eq. (5) and

$C_2 = \frac{k_0}{\left[1 + \frac{K_1}{[H^+]} + \frac{K_1 \cdot K_2}{[H^+]^2}\right]} + \frac{k_1}{\left[1 + \frac{[H^+]}{K_1} + \frac{K_2}{[H^+]}\right]} + \frac{k_2}{\left[1 + \frac{[H^+]}{K_2} + \frac{[H^+]^2}{K_1 \cdot K_2}\right]}$ is from Eq. (10) in $M^{-1} s^{-1}$.

These integrals can be solved analytically if some conditions are met. It is supposed that the concentration of H_2O_2 and O_3 remains constant during the time step. Although the coefficients C_1 and C_2 depend on the pH of the solution (Fig. 2), they can be also considered to be constant during the time step, if time step is small enough. If these conditions are met, the change of the sulfate concentration due to oxidation processes can be given by the following equations:

$$\begin{aligned} \Delta[S(IV)]_1 &= [S(IV)]_{t_0+\Delta t} - [S(IV)]_{t_0} = [S(IV)]_{t_0} \cdot (e^{-C_1[H_2O_2]_{t_0} \cdot \Delta t} - 1) \\ \Delta[S(IV)]_2 &= [S(IV)]_{t_0+\Delta t} - [S(IV)]_{t_0} = [S(IV)]_{t_0} \cdot (e^{-C_2[O_3]_{t_0} \cdot \Delta t} - 1) \\ \Delta[S(IV)] &= \Delta[S(IV)]_1 + \Delta[S(IV)]_2, \end{aligned} \quad (17)$$

where the values of $[S(IV)]$ and $\Delta[S(IV)]$ are in M. The accuracy of these solutions strongly depends on the appropriate choose of the time step. The application of small time step may result in accurate solution, but it significantly reduces the efficiency of the numerical model. Numerical experiments were made to find the appropriate time step.

The calculation of pH is done by the iteration method developed by Hannemann et al. (1995).

3. Results

3.1. Absorption

Fig. 3 shows the time evolution of the pH of water drops at different drop sizes and different composition of the ambient air (see Table 1). (Not all of the

investigated cases are plotted, a few of them were chosen to show the typical time evolution of pH in the water drops.)

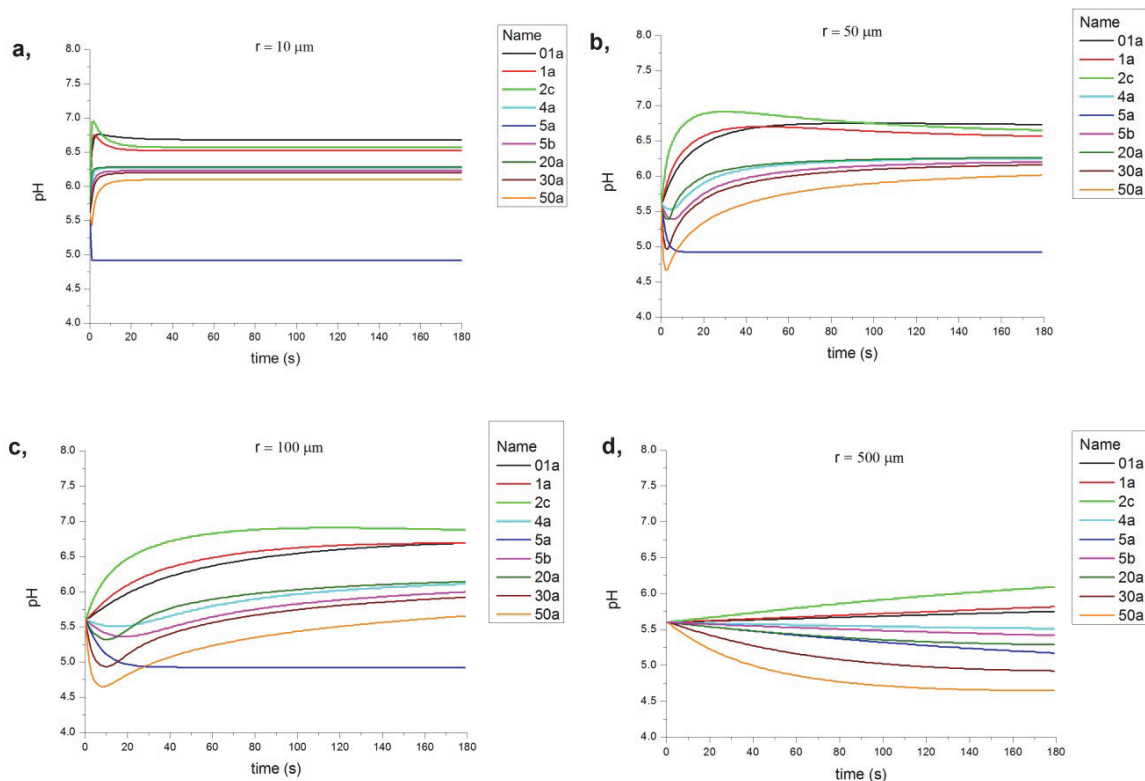


Fig. 3. Time evolution of the pH of the solution at different environmental conditions and different drop sizes: (a) $r = 10 \mu\text{m}$; (b) $r = 50 \mu\text{m}$; (c) $r = 100 \mu\text{m}$, and (d) $r = 500 \mu\text{m}$. The applied time step was equal to 0.01 s in the case of smallest drop size, and it was equal to 0.1 s in the other cases.

In the case of small water drops ($r \leq 20 \mu\text{m}$), the pH of the solution and the concentration of different compounds inside of water drops reach a steady state value in a rather short time period (*Fig. 3a*). This time period is less than 1 s if the concentrations of the trace gases in the ambient air are small, and it remains below 10 s even in the case of extremely polluted atmosphere (concentration of SO_2 and that of NH_3 are high as in the cases of 20a, 30a, 50a). This allows us to suppose that in the case of the small water drops (less than $20 \mu\text{m}$), the concentrations of different compounds are equal to the saturated values.

The presence of NH_3 in the ambient air necessitates the reduction of the time step. The increased sensitivity of the solution on the time step was the consequence of the different dependence of K_H^* of SO_2 and NH_3 on the

concentration of hydrogen ion (*Fig. 1*). If the pH is increasing, the K_H^* of SO_2 is increasing, so SO_2 is getting more efficiently absorbed by water drops. The increased amount of the absorbed SO_2 reduces the pH, which promotes the more efficient absorption of NH_3 gas, and due to the more efficient depletion of NH_3 , the pH of the solute starts to increase. If the time step is not appropriately chosen, the amounts of the absorbed gases are overestimated and, as a consequence, not only the concentration of both SO_2 and NH_3 but also the pH of the solution fluctuate in wide range (*Fig. 4*). As the surface-mass ratio inversely depends on the drop size, the instable solution of Eq. (1) due to the overestimation of the amount of absorbed gases mostly occur in the case of smaller drop sizes ($10\ \mu\text{m}$, $20\ \mu\text{m}$). If the absorption of NH_3 was not taken into consideration (case 5a), longer time step was enough to get stable solution even in the case of the smaller water drops. In this case, the negative feedback between pH and K_H^* of SO_2 controls the absorption of SO_2 .

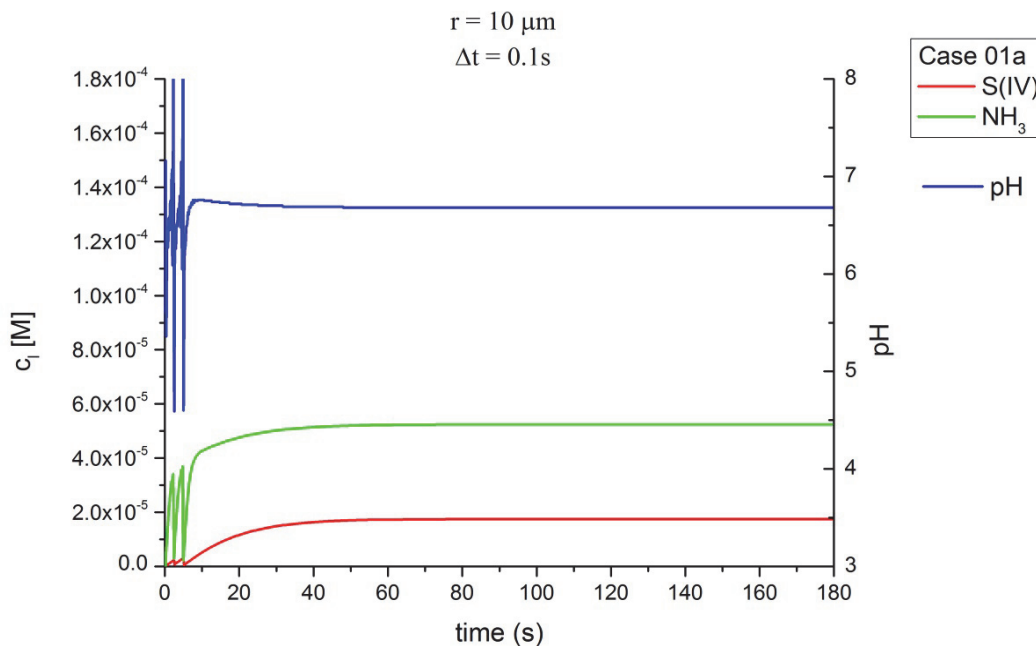


Fig. 4. Time evolution of the pH of the solute (blue curve) and concentration of S(IV) (red curve) and NH_3 (green curve) in the case of the $10\text{-}\mu\text{m}$ -size drop if time step was too long.

In the case of larger drops ($50\ \mu\text{m} \leq r \leq 100\ \mu\text{m}$), the absorption increases the gas concentration with smaller rate than in the case of the smaller ones. Thus, the above mentioned feedback due to absorption of both SO_2 and NH_3 is weaker. If the case when the ambient air does not contain NH_3 (case 5a) is not considered, the pH of solution changes in wider interval in the case of larger drops than in the case of smaller ones. If the environmental conditions are the

same, the pH of the solution in the case of larger drops is smaller compared to the pH of smaller drops. The size dependence of the pH is getting weaker as more SO₂ is absorbed due to the higher concentration of SO₂ in the ambient air (*Figs. 3b* and *c*). If in the environmental air the amount of NH₃ was in excess comparing to SO₂ (01a, 1a, 2c cases), the pH of the solution increased more slowly in time because of the counter effect of the dissolved CO₂ (formation of (CO₂)_{aq}, HCO₃⁻, CO₃²⁻), but it reached a higher value (near 6.5). If SO₂ was in excess, the pH decreased, but it reached constant value in shorter time period. If the absorption of NH₃ was not taken into consideration (case 5a), in the case of drops smaller than 500 μm, the pH of the solution reached a constant value in the first 20 s. This stems from the fact that only gases with acidic properties are absorbed at these environmental conditions. If the atmosphere is strongly polluted (20a, 30a, 50a cases), the evolution of pH is not a monotonic function of time. The pH of the solute decreases in the first 10 s of the simulation, and it starts to increase after reaching the minimum value at about the 10th s of the simulation. The larger the drop size, the longer the time period needed to increase the pH. The value of the pH does not become steady state even by the end of the simulation if the environment is extremely polluted.

In the case of large water drops ($r = 500 \mu\text{m}$), the absorption rate is not large enough to reach the steady state either in the less polluted cases. The pH of the solution continuously decreases during the simulation time, even if only acidic gases were absorbed (*Fig. 3d*). It is interesting to note, that the time evolution of pH is different from the case of smaller drops if the atmosphere is polluted (curves 20a, 30a, 50a). In the cases of smaller drops, the solution becomes rather acidic in a short time period. Later, the pH starts to increase (see *Figs. 3b* and *c*). In the case of larger water drops, the pH continuously decreases during the simulation time getting near to 5.0–4.5 by the end of the simulation (see *Fig. 3d*). The explanation of the dependence of time evolution of pH on the drop size is given in followings:

- (i) Due to its larger concentration in gas phase the absorption of SO₂ gas is the dominant process in the first time period. The sharp decrease of pH (see *Fig. 3b*) significantly increases the absorption rate of NH₃, and near the same amount of both gases were absorbed by the end of the simulation time if drop radius is smaller than 100 μm (*Figs. 5a* and *b*). (Note, that the concentration of SO₂ was larger than that of NH₃ in the ambient air.) The larger concentration of NH₃ inside of the drops finally resulted in larger pH.
- (ii) In the case of larger drops the concentration of neither SO₂ and nor NH₃ become steady state even in the less polluted cases. The absorption of gases is controlled by their chemical properties (furthermore, the pH) and by their concentration in the ambient air. Although NH₃ dissolves better than SO₂, the smaller concentration of NH₃ in the ambient air results in smaller uptake rate if the drop radius is larger than 100 μm.

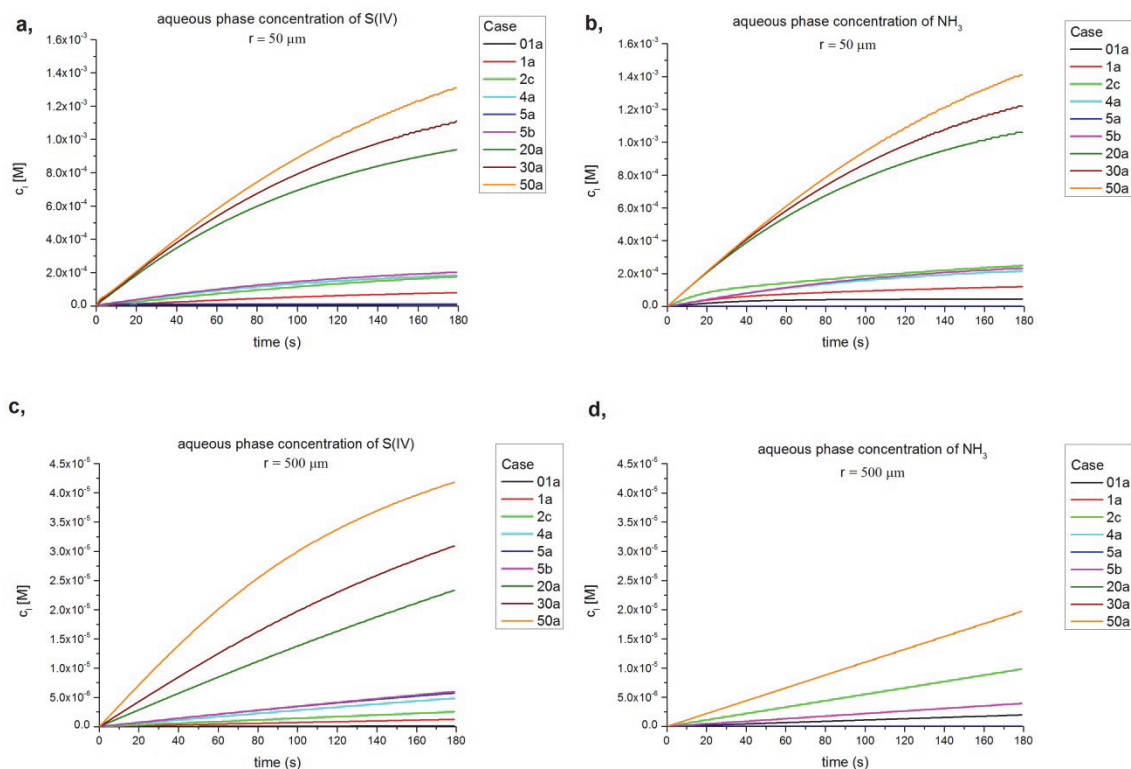


Fig. 5. Time evolution of concentration of S(IV) and NH_3 in the case of two different drop sizes and different environmental conditions.

The analysis of the output data shows (it is not plotted) that aqueous phase concentration of H_2O_2 reaches a constant value in the first 20 s if the radius of the water drop was smaller than $20\ \mu\text{m}$. Its concentration depends on the concentration of the H_2O_2 in the ambient air, and it has not been affected by the presence of the other compounds. This finding corresponds with the independence of the K_H^* of H_2O_2 on the pH of the solution (see Fig. 1). Similar results were found in the case of O_3 . Its concentration increases very fast in the drops, and reaches its maximum value within a few seconds even in the case of water drop with radius of $500\ \mu\text{m}$. The concentration of O_3 does not depend on the concentration of other dissolved gases or on the size of the drop.

3.2. Absorption and oxidation

Smaller time steps comparing with the values in Table 1 were used to avoid the overestimation of the depletion of O_3 due to the oxidation process. The concentration of O_3 inside of the drops was much smaller than the concentration of other species, so the application of too large time step may results in the inaccurate calculation of O_3 . Fig. 6 shows the time evolution of O_3 inside the

water drops with radius of 10 and 50 μm at different time steps. It was found that the time step should be at least 0.001 s to avoid the fluctuation of O_3 concentration caused by the overestimation of the oxidation (see *Figs. 6b* and *d*). The evolution of aqueous phase concentration of O_3 is plotted at greater (0.01 s) and smaller (0.001 s) time steps to demonstrate the fluctuations (*Fig. 6*). In the case of smaller drops significant reduction of the time step was necessary even at lower concentration of sulfate (cases 4a and 5a).

The presence of dissolved NH_3 impacts the aqueous phase concentration of O_3 (*Figs. 6a* and *c*). If there is no NH_3 gas in the ambient air (case 5a), the pH of the solution is smaller, so the oxidation rate by O_3 is also smaller (see *Fig. 2*). In any other cases, O_3 is more efficiently depleted by the oxidation, and its concentration is reduced by about factor of two. Considering the other species, their concentration inside of the water drops is not so sensitive to the value of the time step. The critical time steps defined for absorption were found to be adequate for the numerical integration of the differential equations that describe the oxidation processes if the time evolution of O_3 is not considered.

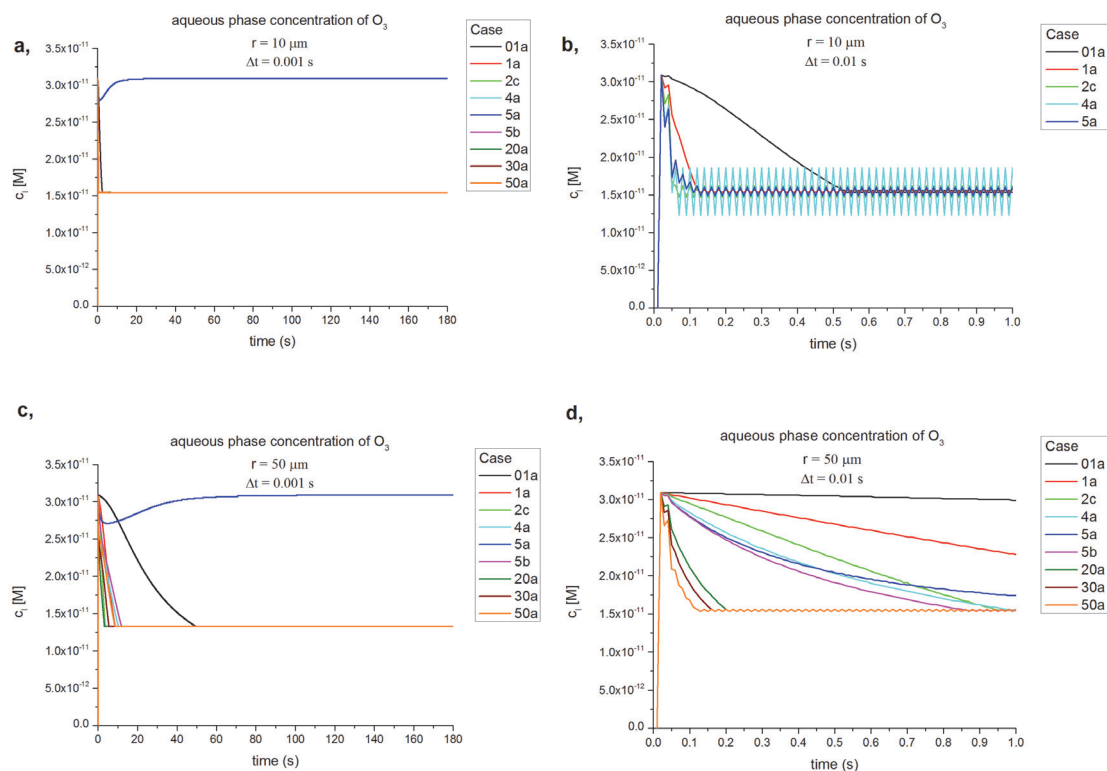


Fig. 6. Time evolution of O_3 at two different drop sizes at time step of 0.01 and 0.001 s. A shorter time period is used for the time evolution of O_3 to demonstrate the effect of too long time step (b, d).

Figs. 7–10 show how the oxidation affects the time evolution of pH and that of the concentration of different compounds in the solution at different drop sizes and different environmental conditions. The results are summarized in the followings:

- (i) The most significant effect can be observed in the case of smallest water drops. If only the absorption is taken into consideration, the pH of the solution becomes constant in a very short time interval. The oxidation of S(IV) significantly impacts the time evolution both of pH and concentrations of different compounds inside of water drops. In the smallest drops, the amount of dissolved SO₂ and NH₃ sharply increases in the first 10–20 s of the simulation (*Figs. 7b* and *c*). By the end of this short time period the concentration of the dissolved H₂O₂ reaches its maximum value, and efficient oxidation of S(IV) to S(VI) results in the reduction of the S(IV). The formation of sulfate results in decrease of pH, and as a consequence, the concentration of the NH₃ further increases. The concentration of H₂O₂ reaches a constant value in a short time period. However, the values of constant concentrations depend on the environmental conditions (*Fig. 7d*). This effect is the consequence of the oxidation. The largest oxidation rate in case 50a results in the smallest H₂O₂ concentration in the water drop. Due to the efficient uptake of H₂O₂ by water drops, the absorption balances the depletion by oxidation at relatively large concentrations (*Fig. 7d*). If SO₂ dominates over NH₃ in the ambient atmosphere, the pH decreases more significantly due to the oxidation. The most dramatic decrease can be observed when no NH₃ gas is present (case 5a). In the other cases, the presence of NH₃ mitigates the decrease of the pH. If NH₃ dominates (case 01a), the efficiency of the oxidation by H₂O₂ is smaller due to the larger pH (see *Fig. 2*), furthermore, the low concentration of O₃ limits the oxidation by O₃.
- (ii) The absence of NH₃ gas in the environment (case 5a) results in very small concentration of S(IV) at each drop size (see *Figs. 7b, 8b, 9b, and 10b*). The low absorption rate of this gas due to the small pH (see *Figs. 7a, 8a, 9a and 10a*) and oxidation by H₂O₂ restrict the accumulation of SO₂ inside water drops.
- (iii) The main characteristics of the time evolutions of concentrations of dissolved compounds hardly depend on the drop size if the drop radius is larger than 20 μm (*Figs. 8–10*). The concentration of the dissolved compounds continuously increases. Except for the extremely polluted cases, even the concentration of H₂O₂ increases during the simulation. The continuous increase of the compounds suggests that the absorption rates exceed the oxidation rates, and it takes longer time to get these processes in balance.

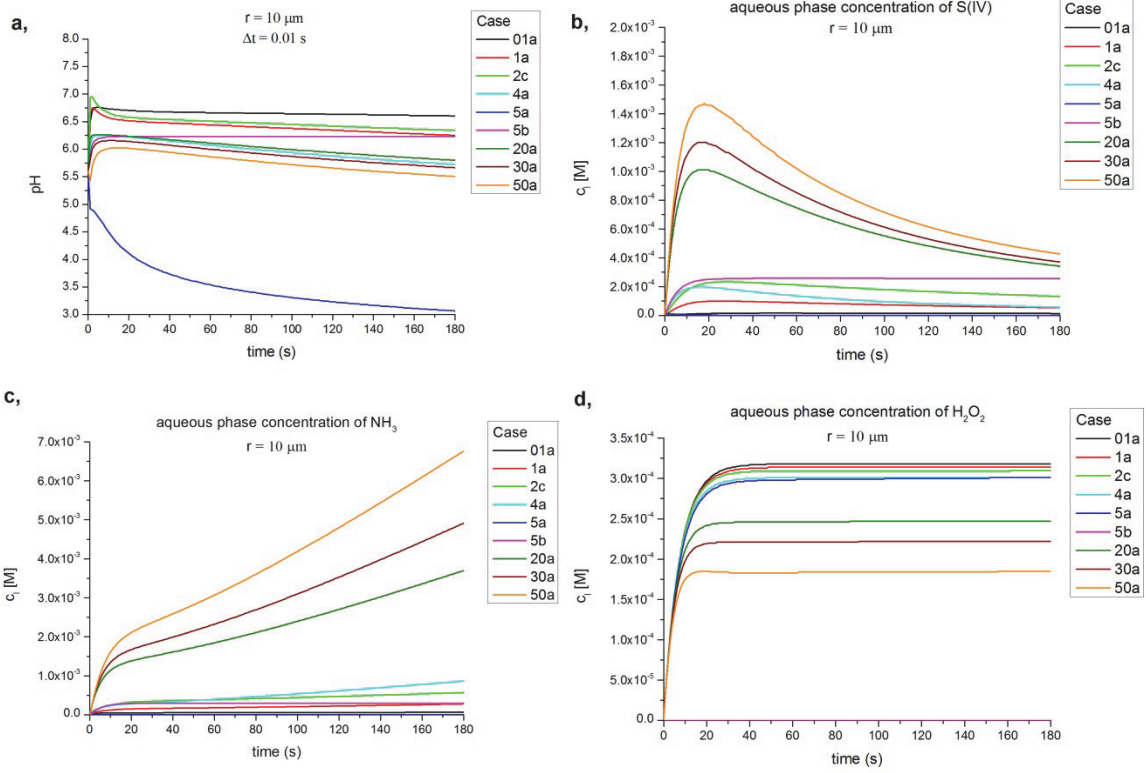


Fig. 7. Time evolution of pH and the concentration of S(IV), NH₃, and H₂O₂ in case of 10 μm drop size (both absorption and oxidation were taken into consideration).

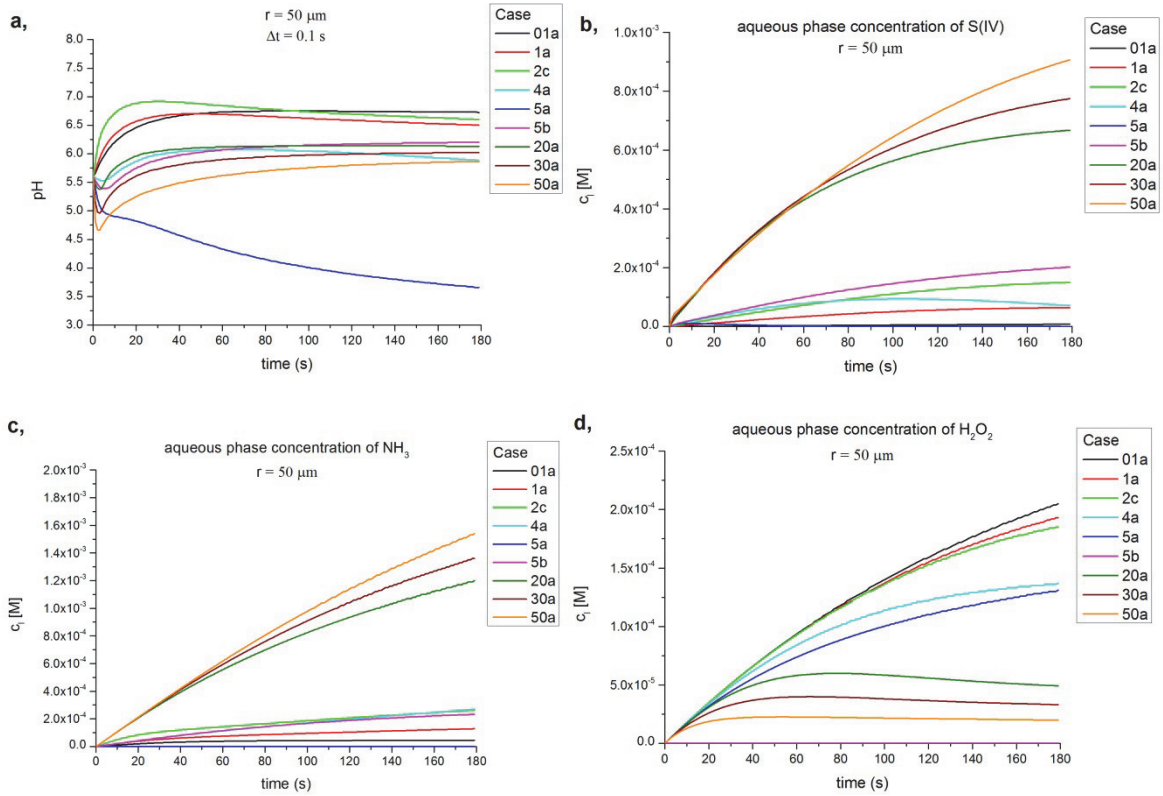


Fig. 8. Same as Fig. 7 for 50 μm drop size.

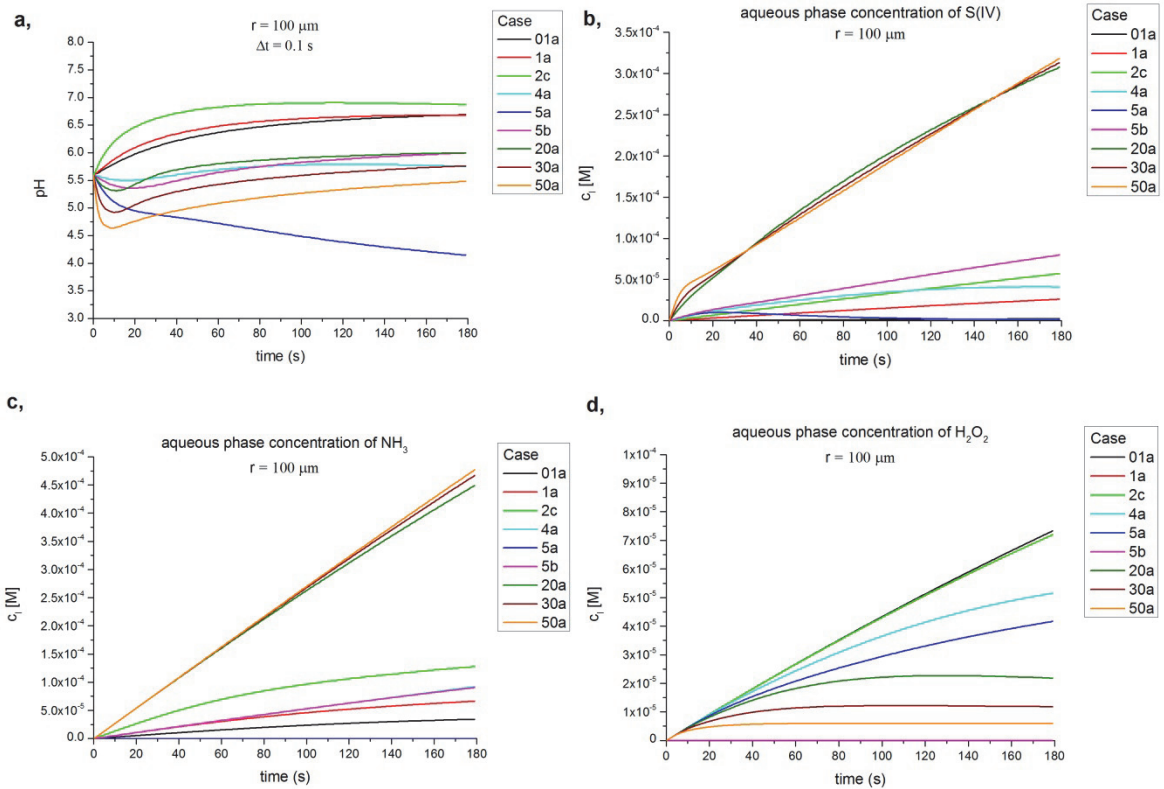


Fig. 9. Same as Fig. 7 for 100 μm drop size.

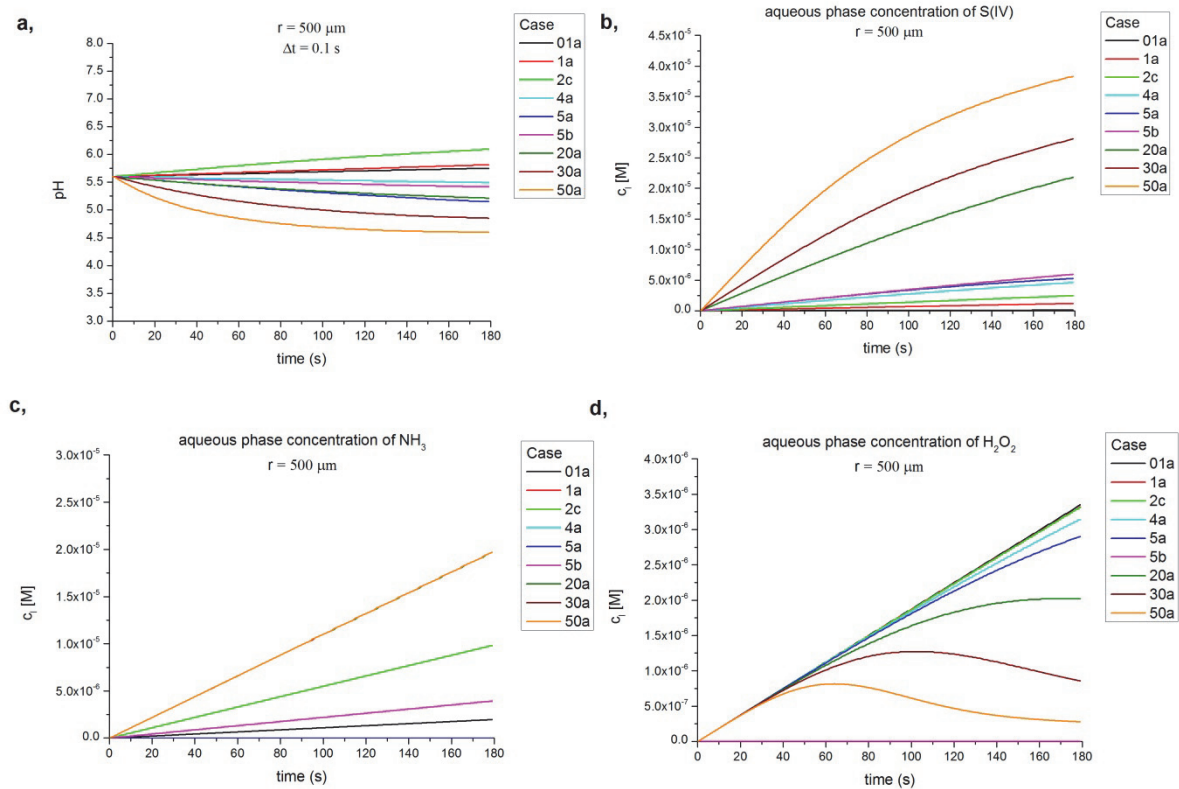


Fig. 10. Same as Fig. 7 for 500 μm drop size.

Fig. 11 shows the time evolution of S(VI) concentrations in water drops at four different drop sizes. The concentrations of S(VI) continuously increase in every case. The fastest increase occurs inside of the smallest drop, and the rate of production of this compound is inversely proportional to the drop size. Another interesting characteristics of the S(VI) production is that the larger the drop size, the larger the delay for the start of the efficient oxidation. While in the case of the smallest drop the concentration of S(VI) starts to increase noticeably after a few seconds, in the case of the largest drop and polluted atmosphere, there is an about 40 s delay. S(VI) formed in the largest concentration in the case of the polluted environment, and the absence of H_2O_2 restrains the formation of S(VI). However, in the case of water drop with radius of $500\ \mu\text{m}$, the sulfate production was constrained by the low SO_2 concentration, rather than by the absence of H_2O_2 (case 5b and case 01a in Fig. 11d).

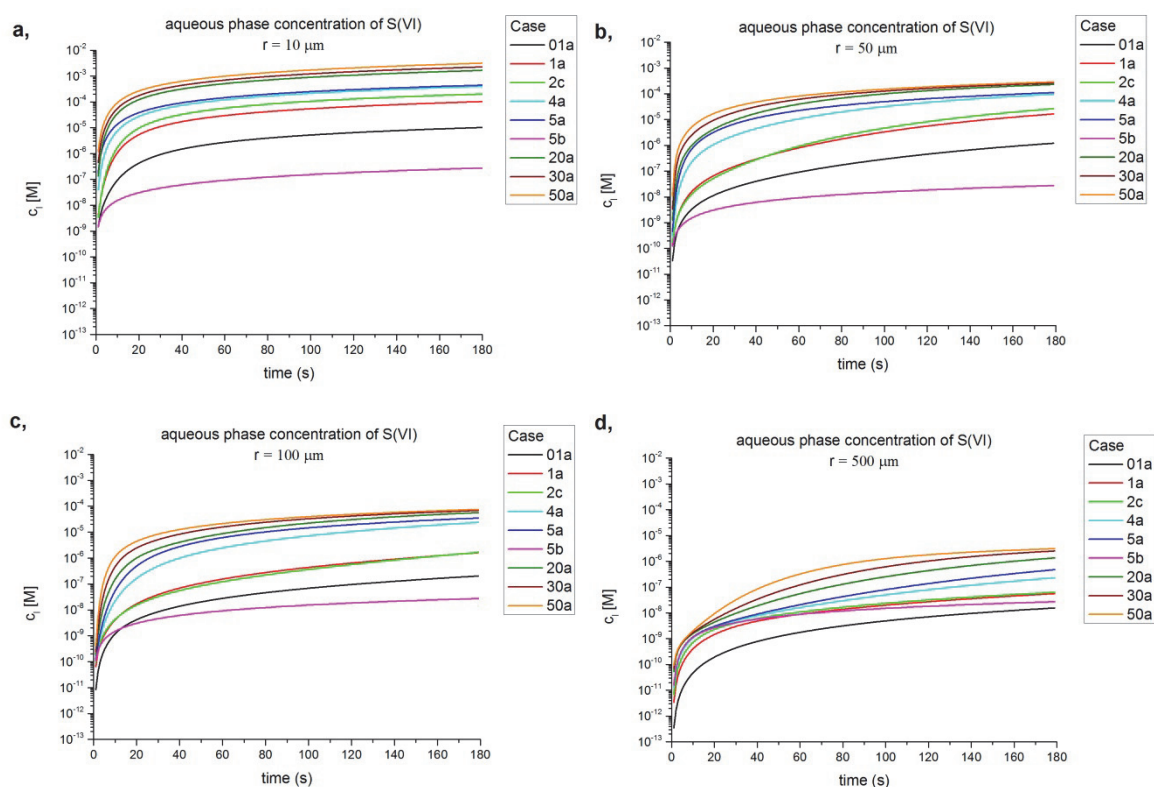


Fig. 11. Time evolution of concentration of S(VI) at different environmental conditions in the case of four different drop sizes.

3.3. Calculation of the produced $(\text{NH}_4)_2\text{SO}_4$

Tables 2–5 summarize the results of the numerical experiments about the oxidation processes (Eq. (16)). The amount of $(\text{NH}_4)_2\text{SO}_4$ is calculated from the final aqueous phase concentrations of SO_4^{2-} and NH_4^+ ions for each drop size and environmental condition (Tables 2–5). Smaller time steps comparing with Table 1 were used during the calculations to obtain the most accurate mass production of $(\text{NH}_4)_2\text{SO}_4$. Except in case when no NH_3 is present in the ambient air (case 5a), the mass of $(\text{NH}_4)_2\text{SO}_4$ formed inside the drops increases with increasing SO_2 gas concentration and with increasing drop size. About one – two order larger amount of ammonium sulfate forms in a polluted atmosphere than in a clean atmosphere. The absence of H_2O_2 (case 5b) had the largest effect on the production of $(\text{NH}_4)_2\text{SO}_4$. If the concentration of H_2O_2 is zero, the $(\text{NH}_4)_2\text{SO}_4$ amount is very small. In this case O_3 becomes the dominant oxidant. Results shows that at environmental conditions used in this research, H_2O_2 is more effective oxidant of S(IV) than O_3 . Significant increase of O_3 concentration in the atmosphere is necessary for the oxidation by O_3 to overwhelm the oxidation by H_2O_2 .

Table 2. Calculated amount of compounds at the end of the simulation in the case of $10\ \mu\text{m}$ drop size

Case	time step [s]	amount of substance [mol]			mass [g]
		SO_4^{2-}	NH_4^+	$(\text{NH}_4)_2\text{SO}_4$	$(\text{NH}_4)_2\text{SO}_4$
01a	0.001	$5.28 \cdot 10^{-17}$	$2.72 \cdot 10^{-16}$	$5.28 \cdot 10^{-17}$	$6.97 \cdot 10^{-15}$
1a	0.01	$4.31 \cdot 10^{-16}$	$1.15 \cdot 10^{-15}$	$4.31 \cdot 10^{-16}$	$5.70 \cdot 10^{-14}$
2c	0.01	$8.50 \cdot 10^{-16}$	$2.39 \cdot 10^{-15}$	$8.50 \cdot 10^{-16}$	$1.12 \cdot 10^{-13}$
4a	0.001	$1.68 \cdot 10^{-15}$	$3.61 \cdot 10^{-15}$	$1.68 \cdot 10^{-15}$	$2.22 \cdot 10^{-13}$
5a	0.01	$2.21 \cdot 10^{-17}$	0.0	0.0	0.0
5b	0.01	$1.16 \cdot 10^{-18}$	$1.24 \cdot 10^{-15}$	$1.16 \cdot 10^{-18}$	$1.54 \cdot 10^{-16}$
20a	0.001	$6.95 \cdot 10^{-15}$	$1.54 \cdot 10^{-14}$	$6.95 \cdot 10^{-15}$	$9.18 \cdot 10^{-13}$
30a	0.001	$9.46 \cdot 10^{-15}$	$2.05 \cdot 10^{-14}$	$9.46 \cdot 10^{-15}$	$1.25 \cdot 10^{-12}$
50a	0.001	$1.32 \cdot 10^{-14}$	$2.82 \cdot 10^{-14}$	$1.32 \cdot 10^{-14}$	$1.74 \cdot 10^{-12}$

Table 3. Same as Table 2 for 50 μm drop size

Case	time step [s]	amount of substance [mol]			mass [g]
		SO_4^{2-}	NH_4^+	$(\text{NH}_4)_2\text{SO}_4$	$(\text{NH}_4)_2\text{SO}_4$
01a	0.01	$7,59 \cdot 10^{-16}$	$2.40 \cdot 10^{-14}$	$7.59 \cdot 10^{-16}$	$1.00 \cdot 10^{-13}$
1a	0.01	$8,63 \cdot 10^{-15}$	$6.75 \cdot 10^{-14}$	$8.63 \cdot 10^{-15}$	$1.14 \cdot 10^{-12}$
2c	0.01	$1,42 \cdot 10^{-14}$	$1.38 \cdot 10^{-13}$	$1.42 \cdot 10^{-14}$	$1.87 \cdot 10^{-12}$
4a	0.01	$5,12 \cdot 10^{-14}$	$1.43 \cdot 10^{-13}$	$5.12 \cdot 10^{-14}$	$6.76 \cdot 10^{-12}$
5a	0.01	$6,06 \cdot 10^{-14}$	0.0	0.0	0.0
5b	0.01	$1,45 \cdot 10^{-16}$	$1.22 \cdot 10^{-13}$	$1.45 \cdot 10^{-16}$	$1.92 \cdot 10^{-14}$
20a	0.01	$1,22 \cdot 10^{-13}$	$6.28 \cdot 10^{-13}$	$1.22 \cdot 10^{-13}$	$1.61 \cdot 10^{-11}$
30a	0.01	$1,39 \cdot 10^{-13}$	$7.17 \cdot 10^{-13}$	$1.39 \cdot 10^{-13}$	$1.83 \cdot 10^{-11}$
50a	0.01	$1,53 \cdot 10^{-13}$	$8.06 \cdot 10^{-13}$	$1.53 \cdot 10^{-13}$	$2.02 \cdot 10^{-11}$

Table 4. Same as Table 2 except for 100 μm drop size

Case	time step [s]	amount of substance [mol]			mass [g]
		SO_4^{2-}	NH_4^+	$(\text{NH}_4)_2\text{SO}_4$	$(\text{NH}_4)_2\text{SO}_4$
01a	0.1	$8.50 \cdot 10^{-16}$	$1.43 \cdot 10^{-13}$	$8.50 \cdot 10^{-16}$	$1.12 \cdot 10^{-13}$
1a	0.1	$6.74 \cdot 10^{-15}$	$2.78 \cdot 10^{-13}$	$6.74 \cdot 10^{-15}$	$8.91 \cdot 10^{-13}$
2c	0.1	$6.95 \cdot 10^{-15}$	$5.35 \cdot 10^{-13}$	$6.95 \cdot 10^{-15}$	$9.18 \cdot 10^{-13}$
4a	0.01	$1.03 \cdot 10^{-13}$	$3.88 \cdot 10^{-13}$	$1.03 \cdot 10^{-13}$	$1.36 \cdot 10^{-11}$
5a	0.01	$1.49 \cdot 10^{-13}$	0.0	0.0	0.0
5b	0.01	$1.16 \cdot 10^{-15}$	$3.82 \cdot 10^{-13}$	$1.16 \cdot 10^{-15}$	$1.53 \cdot 10^{-13}$
20a	0.01	$2.42 \cdot 10^{-13}$	$1.89 \cdot 10^{-12}$	$2.42 \cdot 10^{-13}$	$3.20 \cdot 10^{-11}$
30a	0.01	$2.92 \cdot 10^{-13}$	$1.97 \cdot 10^{-12}$	$2.92 \cdot 10^{-13}$	$3.86 \cdot 10^{-11}$
50a	0.01	$3.22 \cdot 10^{-13}$	$2.01 \cdot 10^{-12}$	$3.22 \cdot 10^{-13}$	$4.25 \cdot 10^{-11}$

Table 5. Same as Table 2 except for 500 μm drop size

Case	time step [s]	amount of substance [mol]			mass [g]
		SO_4^{2-}	NH_4^+	$(\text{NH}_4)_2\text{SO}_4$	$(\text{NH}_4)_2\text{SO}_4$
01a	0.1	$8.16 \cdot 10^{-15}$	$1.03 \cdot 10^{-12}$	$8.16 \cdot 10^{-15}$	$1.08 \cdot 10^{-12}$
1a	0.1	$2.93 \cdot 10^{-14}$	$2.06 \cdot 10^{-12}$	$2.93 \cdot 10^{-14}$	$3.87 \cdot 10^{-12}$
2c	0.1	$3.29 \cdot 10^{-14}$	$5.14 \cdot 10^{-12}$	$3.29 \cdot 10^{-14}$	$4.34 \cdot 10^{-12}$
4a	0.1	$1.21 \cdot 10^{-13}$	$2.06 \cdot 10^{-12}$	$1.21 \cdot 10^{-13}$	$1.60 \cdot 10^{-11}$
5a	0.1	$2.49 \cdot 10^{-13}$	0.0	0.0	0.0
5b	0.1	$1.43 \cdot 10^{-14}$	$2.06 \cdot 10^{-12}$	$1.43 \cdot 10^{-14}$	$1.89 \cdot 10^{-12}$
20a	0.1	$7.11 \cdot 10^{-13}$	$1.03 \cdot 10^{-11}$	$7.11 \cdot 10^{-13}$	$9.40 \cdot 10^{-11}$
30a	0.1	$1.32 \cdot 10^{-12}$	$1.03 \cdot 10^{-11}$	$1.32 \cdot 10^{-12}$	$1.75 \cdot 10^{-10}$
50a	0.1	$1.62 \cdot 10^{-12}$	$1.03 \cdot 10^{-11}$	$1.62 \cdot 10^{-12}$	$2.15 \cdot 10^{-10}$

4. Conclusions

A box model was developed to simulate absorption and chemical reactions that occur inside water drops. The purpose of the research was to investigate how sulfate formation depends on the drop size, and to find efficient scheme for the numerical integration of ODEs which describe absorption and chemical reactions. To focus on these processes, the diffusional growth of water drops and the accretion by collision-coalescence were not taken into consideration. Results are summarized in the followings:

- (i) The accurate solution of the differential equations describing the absorption of gases through the surface of water drops needs rather small time step. The value of the critical time step depends on the environmental conditions and the size of the drop. The presence of NH_3 in the ambient air reduces the value of the critical time step. As a rule of thumb, time step of 0.01 s is suggested to apply if the drop radius is smaller than 20 μm , and of 0.1 s if the drop radius is above this size.
- (ii) The numerical solution of the differential equations needs further reduction of the time step if the concentration of one of reacting compounds is small comparing to the other compounds.
- (iii) The time evolution of pH and that of the concentration of different species depends on the drops size. In the case of small water drops, both the pH of the solution and the concentration of the chemical compounds become steady state in a short time period of about 10 s. In the case of the larger drops, this time period can become significantly longer depending on the pollution of the ambient air and on the drop size. The only exception is the concentration of H_2O_2 . The concentration of this gas becomes steady state before the end of the simulation even in the extremely polluted cases.
- (iv) The oxidation significantly impacts the amount of absorbed gases. The reduction of pH due to the formation of sulfate slightly increase the amount of absorbed NH_3 , and the depletion of S(IV) and H_2O_2 by oxidation allows further absorption of both SO_2 and H_2O_2 gases. While in the case of drops with size of 10 μm , the absorptions and chemical reactions get into balance during the simulated time period, in the case of larger drops, the concentration of different species continuously increases.
- (iv) The sulfate formation is significantly impacted by the environmental conditions and the drop size. The fastest increase of mole concentration of sulfate occurs inside the smallest drop, and the rate of increase is the smallest in the cases of the largest drop.
- (v) Significant amount of ammonium sulfate can be produced by oxidation inside of water drops, which increases the mass of the CCN after the evaporation of water drops. In the case of polluted atmosphere, the mass of

ammonium sulfate formed by this way is comparable to the mass of CCN that the drops formed on.

- (vi) Strong size dependence of sulfate production suggests that application of the bin microphysical scheme may give a more accurate description of the chemical processes than the bulk schemes which are currently used to simulate these processes. The application of the bin scheme is limited by the large computer capacity required by this scheme.

In the next phase of the research, these results will be applied to simulate the absorption and chemical reactions in stratocumulus clouds by using two-dimensional cloud model with bin microphysical scheme.

Acknowledgment: The contribution to this research by *I. Geresdi* was supported by Hungarian Scientific Research Found (Number: OTKA K116025).

References

- Barrie, L.A. and Georgii, H.W., 1976:* An experimental investigation of the absorption of sulfur dioxide by water drops containing heavy metal ions. *Atmos. Environ.* 10, 743–749.
- Barrie, L.A., 1985:* Features of the atmospheric cycle of aerosol trace elements and sulfur dioxide revealed by baseline observations in Canada. *J. Atmos. Chem.* 3, 139–152.
- Beilke, S. and Georgii, H.W., 1968:* Investigation on the incorporation of sulfur dioxide into fog and raindrops. *Tellus* 20, 435–441.
- Beilke, S., 1970:* Laboratory investigations of washout trace gases. In (Eds.: *Engelmann, R.J. and Slinn, W.G.N.*) *Precipitation Scavenging (1970)*. U.S. Atomic Energy Commission, AEC symposium series 22, 261–267.
- Beilke, S., Lamb, D. and Müller, J., 1975:* On the oxidation of SO₂ in aqueous systems. *Tellus* 20, 435–441.
- Daum, P.H., Schwartz, S.E. and Newman, L., 1983:* Studies of the gas and aqueous phase composition of stratiform clouds. In (Eds.: *Pruppacher, H.R., Semonin, R.G. and Slinn, W.G.N.*) *Precipitation Scavenging, Dry Deposition, and Resuspension, Volume 1*. Elsevier Science Publishing Co., New York, 31–51.
- Diehl, K., Mitra, S.K. and Pruppacher, H.R., 1998:* A laboratory study on the uptake of HCl, HNO₃ and SO₂ gas by ice crystals and the effect of these gases on the evaporation rate of the crystals. *Atmos. Res.* 47–48, 235–244.
- Diehl, K., Vohl, O., Mitra, S. K. and Pruppacher, H. R., 2000:* A laboratory and theoretical study on the uptake of sulfur dioxide gas by small water drops containing hydrogen peroxide under laminar and turbulent conditions. *Atmos. Environ.* 34 2865–2871.
- Diehl, K., Mitra, S. K., Szakáll, M., v. Blohn, N. , Borrmann, S. and Pruppacher, H.R., 2011:* The Mainz Vertical Wind Tunnel facility—a review of 25 years of laboratory experiments on cloud physics and chemistry. In (Eds.: *Justin D. Pereira*) *Wind Tunnels: Aerodynamics, Models and Experiments*. Nova Science Publishers, United States.
- Geresdi, I. and Weidinger, T., 1989:* A meteorológiai folyamatok modellezésében alkalmazott numerikus módszerek. *Időjárás* 93, 100–114.
- Hannemann, A., 1995:* Eine experimentelle und theoretische Untersuchung zur gekoppelten ufnahme von NH₃, CO₂ und SO₂ in Wassertropfen. Zugl. Mainz, Universität, Diss., Shaker Verlag GmbH, Aachen.
- Hannemann, A.U., Mitra, S.K. and Pruppacher, H.R., 1995:* On the Scavenging of Gaseous Nitrogen Compounds by Large and Small Rain Drops I. A Wind Tunnel and Theoretical Study of the Uptake and Desorption of NH₃ in the Presence of CO₂. *J. Atmos. Chem.* 21, 293–307.

- Hannemann, A.U., Mitra, S.K. and Pruppacher, H.R., 1996: On the Scavenging of Gaseous Nitrogen Compounds by Large and Small Rain Drops: II. Wind Tunnel and Theoretical Studies of the simultaneous Uptake of NH_3 , SO_2 and CO_2 by Water Drops. *J. Atmos. Chem.* 24, 271–284.
- Hegg, D.A. and Hobbs, P.V., 1981. Cloud water chemistry and chemical production of sulfates in clouds. *Atmos. Environ.* 15, 1597–1604.
- Hegg, D.A. and Hobbs, P.V., 1982. Measurements of sulfate production in natural clouds. *Atmos. Environ.* 16, 2663–2668.
- Hegg, D.A., Hobbs, P.V. and Raschke, L.F., 1984: Measurements of the scavenging of sulfate and nitrate in clouds. *Atmos. Environ.* 18, 1939–1946.
- Hoffmann, M.R. and Calvert, J.G., 1985: Chemical Transformation Modules for Eulerian Acid Deposition Models, Vol. 2, The Aqueous-Phase Chemistry, EPA/600/3-85/017, U.S. Environmental Protection Agency, Research Triangle Park, NC.
- Horváth, L., 1977: A légköri kén-dioxid szulfáttá alakulásának mechanizmusa és kinetikája. *Időjárás* 81, 5, 280–287. (In Hungarian)
- Horváth, L. and Mészáros, E., 1978: Determination of the kinetic parameters of sulfur-dioxide - sulfate conversion on the basis of atmospheric measurements. *Időjárás* 82, 2, 58–62.
- Horváth, L., 1981: A csapadékvíz kémiai összetétele Magyarországon. *Időjárás* 85, 4, 201–212. (In Hungarian)
- Johnson, A.I., Hamielec, A.E. and Houghton, W.T., 1967: An experimental study of mass transfer with chemical reaction from single gas bubbles. *Canadian J. Chem. Engin.* 45, 140–144.
- Kronig, R. and Brink, J.C., 1950: On the theory of the extraction from falling drops, *J. Appl. Sci. Res.* A2, 142–154.
- Kronig, R., Vanderveen, B. and Ijzerman, P., 1951: On the theory of extraction from falling droplets. II. *J. Appl. Sci. Res.* A3, 103–110.
- McArdle, J.V. and Hoffmann, M.R., 1983: Kinetics and mechanism of the oxidation of aquated sulfur dioxide by hydrogen peroxide at low pH. *J. Phys. Chem.* 87, 5425–5429.
- Mészáros, Á. and Vissy, K., 1974: Concentration, size distribution and chemical nature of atmospheric aerosol particles in remote oceanic areas. *J. Aerosol Sci.* 5, 101–110.
- Mészáros, E., 1971: The size distribution of water soluble particles in the atmosphere. *Időjárás* 75, 308–314.
- Mészáros, E., 1973: Evidence of the role of indirect photochemical processes in the formation of atmospheric sulphate particulate. *J. Aerosol Sci.* 4, 429–434.
- Mészáros, E., 1974: On the formation of atmospheric sulphate particulate in the winter months. *J. Aerosol Sci.* 5, 483–485.
- Mészáros, E., Sas, É. and Mészáros, Á., 1974: Felhőcseppek kondenzációs növekedése ammónium-szulfát magvakon. *Időjárás* 78, 333–341.
- Mészáros, E. and Várhelyi, G., 1975: On the concentration, size distribution and residence time of sulfate particles in the lower troposphere. *Időjárás* 79, 267–273.
- Mészáros, E., 1976: A kén körforgalma a légkörben. *Időjárás* 80, 1, 42–47. (In Hungarian)
- Mitra, S.K. and Hannemann, A.U., 1993: On the Scavenging of SO_2 by Large and Small Rain Drops: V. A Wind Tunnel and Theoretical Study of the Desorption of SO_2 from Water Drops Containing S(IV). *J. Atmos. Chem.* 16, 201–218
- Mitra, S.K., Waltrip, A., Hannemann, A., Flossmann, A. and Pruppacher, H.R., 1992: A wind tunnel and theoretical investigation to test various theories for the absorption of SO_2 by drops of pure water and water drops containing H_2O_2 and $(\text{NH}_4)_2\text{SO}_4$. In: Schwartz, S.E. and Slinn, W.G.N. (eds.), *Precipitation Scavenging and Atmosphere – Surface Exchange*, Vol. 1. Hemisphere Publishing, Washington, DC, 123–141.
- Pruppacher, H.R. and Klett, J.D., 2010: *Microphysics of Clouds and Precipitation*. Second revised and expanded edition, Springer Science+Business Media B.V., Springer Dordrecht Heidelberg London New York.
- Seinfeld, J.H. and Pandis, S.N., 2006: *Atmospheric Chemistry and Physics*. John Wiley & Sons, Inc., Hoboken, New Jersey
- Seinfeld, J.H., 1986: *Atmospheric Chemistry and Physics of Air Pollution*. John Wiley & Sons, Inc., New Jersey.

- Stuart, A.L. and Jacobson, M.Z., 2006: A Numerical Model of the Partitioning of Trace Chemical Solutes during Drop Freezing. *J. Atmos. Chem.* 53 (2006), 13–42
- Várhelyi, G., 1977: Wet removal of tropospheric sulfur compounds. *Időjárás* 81, 85–93.
- Várhelyi, G., 1980: Dry deposition of atmospheric sulfur and nitrogen oxides. *Időjárás* 84, 15–20.
- Várhelyi, G., 1982: On the atmospheric sulfur budget over Hungary. *Időjárás* 86, 333–337.
- Várhelyi, G., 1975: A kén-dioxid abszorpciója és oxidációja felhő- és ködcspepekben. *Időjárás* 79, 360–365. (In Hungarian)
- v. Blohn, N., Diehl, K., Nölscher, A., Jost, A., Mitra, S. K. and Borrmann, S., 2013: The retention of ammonia and sulfur dioxide during riming of ice particles and dendritic snow flakes: laboratory experiments in the Mainz vertical wind tunnel. *J. Atmos. Chem.* 70, 131–150.
- Walcek, C.J. and Pruppacher, H.R., 1984: On the scavenging of SO₂ by cloud and rain drops. I: a theoretical study of SO₂ absorption and desorption for water drops in air. *J. Atmos. Chem.* 1, 269–289.
- Waltrop, A., Mitra, S.K., Flossmann, A.I. and Pruppacher, H.R., 1991: On the scavenging of SO₂ by cloud and rain drops: IV. A wind tunnel and theoretical study on the adsorption of SO₂ in the ppb(v) range by water drops containing H₂O₂. *J. Atmos. Chem.* 12, 1–17.
- Watada, H., Hamielec, A.E. and Johnson, A.I., 1970: A theoretical study of mass transfer with chemical reaction in drops. *Canadian J. Chem. Engin.* 48, 255–261.